A&A 405, 505–511 (2003)
DOI: 10.1051/0004-6361:20030638

Astronomy & Astrophysics

RX J0042.3+4115: A stellar mass black hole binary identified in M 31

R. Barnard[1], J. P. Osborne[2], U. Kolb[1], and K. N. Borozdin[3]

[1] The Department of Physics and Astronomy, The Open University, Walton Hall, Milton Keynes, MK7 6BT, UK
[2] The Department of Physics and Astronomy, The University of Leicester, Leicester, LE1 7RH, UK
[3] Los Alamos National Laboratory, PO Box 1663, Mail Stop D436, NIS-2, Los Alamos, MN 87545, USA

Received 6 February 2003 / Accepted 17 April 2003

Abstract. Four XMM-Newton X-ray observations of the central region of the Andromeda Galaxy (M 31) have revealed an X-ray source that varies in luminosity over $\sim 1\text{–}3 \times 10^{38}$ erg s^{-1} between observations and also displays significant variability over time-scales of a few hundred seconds. The power density spectra of lightcurves obtained in the 0.3–10 keV energy band from the three EPIC instruments on board XMM-Newton are typical of disc-accreting X-ray binaries at low accretion rates, observed in neutron star binaries only at much lower luminosities ($\sim 10^{36}$ erg s^{-1}). However X-ray binaries with massive black hole primaries have exhibited such power spectra for luminosities $>10^{38}$ erg s^{-1}. We discuss alternative possibilities where RX J0042.3+4115 may be a background AGN or foreground object in the field of view, but conclude that it is located within M 31 and hence use the observed power spectra and X-ray luminosities to identify the primary as a black hole candidate.

Key words. X-rays: general – galaxies: individual: M 31 – X-rays: binaries – black hole physics

1. Introduction

At 760 kpc (van den Bergh 2000) the Andromeda Galaxy (M 31) is the nearest spiral galaxy to our own. The X-ray emission from the direction of M 31 is dominated by point sources, mostly X-ray binaries (XB), with a mixture of supernova remnants, foreground stars and background AGN. The intensity variations on short and long time-scales in the X-ray sources in M 31 provide vital clues to their nature, and in some cases, in combination with X-ray spectral information, they can be classified from the X-ray observations alone. The study of variability in X-ray sources in external galaxies has been limited by the sensitivity of previous observatories, but the three large X-ray telescopes on board XMM-Newton make such a project possible down to a luminosity of $\sim 10^{36}$ erg s^{-1}; the combined effective area of these telescopes is the largest of any X-ray telescope imaging above 2 keV. A recent Chandra survey has revealed that ~50% of the X-ray sources in M 31 vary over long time-scales (Kong et al. 2002), several transients have been discovered in XMM-Newton observations (e.g. Trudolyubov et al. 2001 2002b; Osborne et al. 2001) and periodic dipping was observed with XMM-Newton in the M 31 globular cluster source Bo158 by Trudolyubov et al. (2002a).

Send offprint requests to: R. Barnard,
e-mail: r.barnard@open.ac.uk

The J2000 X-ray position of RX J0042.3+4115, named following Supper et al. (1997) but first identified by Trinchieri & Fabbiano (1991), was determined to be $00^{\rm h}\,42^{\rm m}\,22\overset{\rm s}{.}919\ +41^\circ\,15'\,35\overset{''}{.}14$ in a recent Chandra survey of M 31 (Kong et al. 2002). It was not associated with known supernova remnants, foreground objects, globular clusters or background galaxies (Kong et al. 2002). RX J0042.3+4115 shows luminosities in the 0.3–10 keV band of a few 10^{38} erg s^{-1}, and significant variations in colour and intensity over time-scales of a few hundred seconds (Sect. 5); in our galaxy, such behaviour is exhibited in only a handful of XB, all of which are bright microquasars with neutron star primaries (Z-sources, e.g. Hasinger & van der Klis 1989; Fender 2002) or transient microquasars with suspected black hole primaries (e.g. Belloni et al. 2000; Fender 2002).

In this paper we propose that RX J0042.3+4115 is a black hole binary. The case is summarised below and expounded in the subsequent sections. The power density spectra (PDS) of the ~200 Galactic disc-accreting X-ray binaries (XB) are determined by their accretion rates, and hence luminosities; nearly all disc accreting XB are low mass X-ray binaries (LMXB), but some high mass X-ray binaries (e.g. Cygnus X-1) also exhibit disc accretion. The PDS of low accretion rate, disc accreting XB are approximately flat at frequencies <0.01–1 Hz, then break to a steep power law; these characteristics are present irrespective of the primary (Wijnands & van der Klis 1999). At high accretion rates the PDS are varied but are distinct from

the low accretion rate PDS in that the low frequency noise is described by a power law without the break (Hasinger & van der Klis 1989). In Galactic neutron star LMXB, low accretion rate PDS are seen in sources with luminosities of a few 10^{36} erg s^{-1}; in contrast we find that RX J0042.3+4115 exhibits a low accretion rate PDS at luminosities of ~ 1–3×10^{38} erg s^{-1}. This is close to the Eddington luminosity of an accreting neutron star ($\sim 2 \times 10^{38}$ erg s^{-1}, Frank et al. 2002). If RX J0042.3+4115 was a neutron star binary, a high accretion rate would be required for the observed luminosity and the characteristic low accretion rate PDS would not be seen. Hence, the primary in RX J0042.3+4115 is unlikely to be a neutron star and so must be a black hole.

The next section reviews the properties of Galactic black hole binaries to provide a context for the subsequent discussion. A summary of observations and analysis techniques follows, then the luminosities and power spectral breaks observed in RX J0042.3+4115 are presented in Sect. 5. The case for a black hole primary in RX J0042.3+4115 is presented in the final section.

2. Galactic black hole binaries

Black hole binaries can be classified as persistent or transient, and each can exist in any one of three states- the low/hard state, the high/soft state and intermediate/very high state. The X-ray spectrum in the high/soft state is black-body dominated, while the low/hard spectrum is dominated by a power law with a spectral index ∼1.5. The intermediate/high state exhibits strong black body and power law features. As suggested by their names, these states were originally supposed to be related to the mass accretion rate and hence luminosity; however, the same "state" can be observed at extremely different flux levels (e.g. Homan et al. 2001). The four Galactic persistent black hole binaries (Cygnus X-1, GX 399−4, 1E 1740.7−2942 and GRS 1758−258) spend most of their time in their low/hard state (Fender 2002, and references within). Meanwhile, transient black hole binaries can switch states very rapidly; Belloni et al. (2000) have identified 12 separate classes of behaviour in the microquasar GRS 1915+105 which involve transitions between two or all three of the states.

Microquasars are compact accreting binary systems with low mass secondary stars that exhibit relativistic outflows, or jets; the similarity with quasars gives them their name (Fender 2002). Relativistic jets from binaries were first discovered in SS 433 (Spencer 1979; Hjellming & Johnston 1981a,b), and have since been discovered in ∼30 Galactic XB (Fender 2002); 11 microquasars are neutron star binaries and 19 are black hole binaries (Fender 2002). As yet, the only Galactic black hole binaries to exhibit luminosities $>10^{38}$ erg s^{-1} have been microquasars. Hence, they may be the closest Galactic analogue to RX J0042.3+4115.

3. The observations

Four observations were made of the core of M 31 with XMM-Newton; data were analysed from the three imaging instruments, one PN (Strüder et al. 2001) and two MOS (Turner et al. 2001), which share a common circular field-of view with a 30′ diameter (Jansen et al. 2001). The MOS detectors have a usable energy range of 0.3–10 keV, a point spread function FWHM of 5″, an energy resolution of ∼70 eV and a time resolution of 2.6 s in the "full frame" mode used for these observations (Turner et al. 2001). The PN detector has broadly similar characteristics, but with approximately twice the effective area of an individual MOS. Full frame mode was used, giving a time resolution of 0.0734 s (Strüder et al. 2001). The combined effective area is ∼2400 cm^2 at 1 keV (Jansen et al. 2001). A journal of the XMM-Newton observations is given in Table 1, which details the date, duration and filter used for each observation.

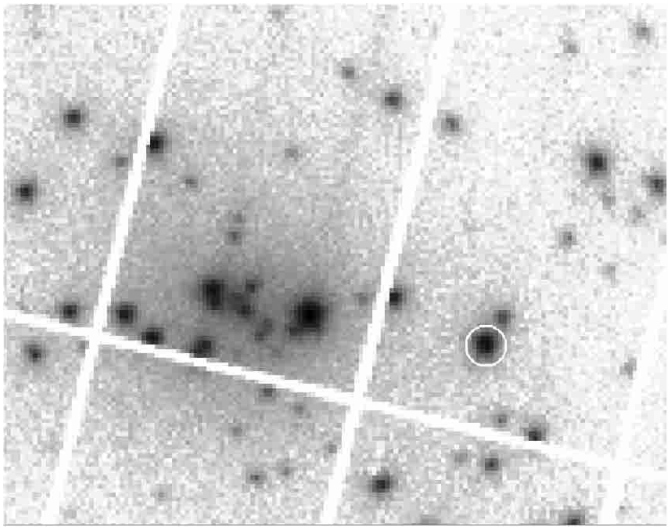

Fig. 1. A detail of the 0.3–10 keV PN image from the June 2001 XMM-Newton observation of the core of M 31; north is up, east is left. The image is 11′ across, its intensity is log scaled. RX J0042.3.9+4115 is circled in white, the circle defining the source extraction region.

Table 1. Journal of XMM-Newton observations of the M 31 core.

Observation	Date	Duration	Filter
1 (rev 0100)	25 July 2000	34 ks	Medium
2 (rev 0193)	27 December 2000	13 ks	Medium
3 (rev 0285)	29 June 2001	56 ks	Medium
4 (rev 0381)	6 January 02	61 ks	Thin

4. Analysis

Lightcurves were obtained in the 0.3–2.5, 2.5–10 and 0.3–10 keV energy bands, at 0.0734 s resolution from the PN and 2.6 s resolution from the MOS cameras. The data were filtered to select only good events (FLAG = 0) with SAS version 5.3.3[1] and analysed with the HEASOFT utility suite[2]; only events in the energy band 0.3–10 keV with PATTERN < 4 or 12, for PN and MOS respectively, were

[1] http://heasarc.gsfc.nasa.gov/docs/xmm/uhb/

[2] http://heasarc.gsfc.nasa.gov/docs/software/lheasoft/

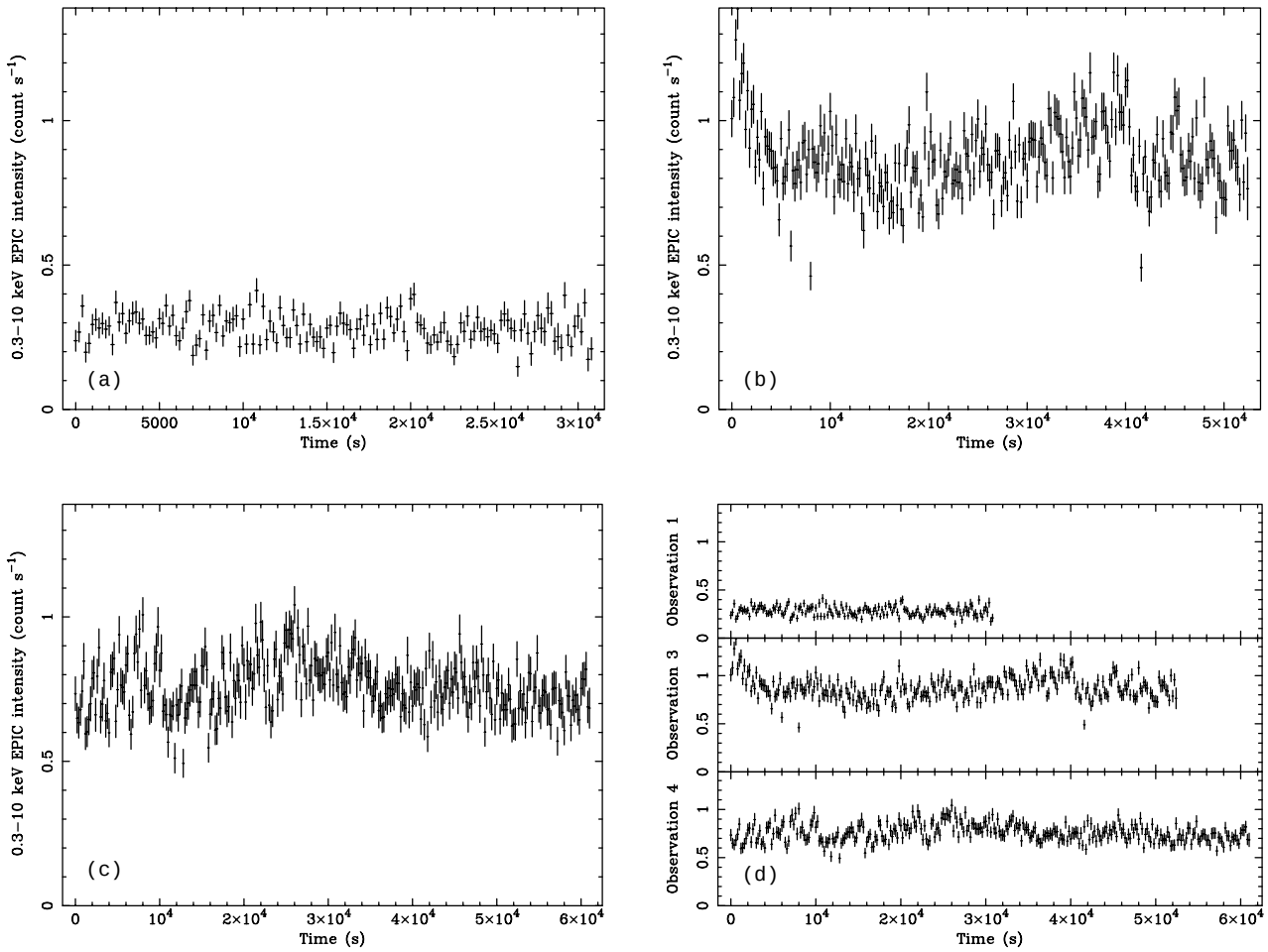

Fig. 2. Combined EPIC lightcurves of RX J0042.3+4115 in the 0.3–10 keV energy band from observations 1 **a**), 3 **b**) and 4 **c**); the lightcurves have 200 s binning. The χ^2/d.o.f. for the best fit lines of constant intensity for observations 1, 3 and 4 are 287/154, 329/125 and 798/306 respectively. Although each lightcurve is highly variable, there appears to be no pattern to their behaviour. The three lightcurves are presented with the same time and intensity scales in **d)** for easier comparison.

selected. Background flaring was present in observations 1, 3 and 4, and so intervals in which the total PN count rate exceeded 60 count s^{-1} or the count rate of a single MOS detector exceeded 30 count s^{-1} were rejected; only observation 3 exceeded these thresholds, reducing the useful exposure to 27 ks. There are ∼120 X-ray point sources in the field of view, and the extraction regions for our source was limited to 20″ to avoid contamination by a neighbouring point source; this encircles ∼70% of the flux. The PN image of the Core of M 31 from the June 2001 XMM-Newton observation is shown in Fig. 1 with RX J0042.3+4115 circled.

For each lightcurve on source, a source-free background lightcurve was extracted from a nearby region on the same CCD and at a similar off-axis angle, the same filtering criteria were used. The fractional exposure of the source was estimated from the exposure map, and the lightcurves were corrected for the overall effects of deadtime and vignetting using FCALC.

Additionally, PN source and background spectra were obtained from all good-time data for observations 1, 3 and 4; in observation 2, the source fell in a chip gap. Response matrices and ancillary response files were generated for each spectrum, with RMFGEN and ARFGEN respectively. The spectra were grouped to have a minimum of 50 counts per bin, data below 0.3 keV or greater than 10 keV were ignored in the subsequent analysis.

5. Results

The combined, exposure corrected, background subtracted 0.3–10 keV EPIC lightcurves of RX J0042.3+4115 from observations 1, 3 and 4 are presented in Fig. 2; these lightcurves are clearly variable, but display no regular behaviour. The lightcurves vary by ∼30% within each observation, while the mean intensity of the lightcurve from observation 1 is a factor of ∼3 lower than the mean intensities in observations 3 and 4. Estimates of the luminosity of RX J0042.3+4115 in each observation were obtained by fitting the background-subtracted PN spectra with three simple models. Model A is a simple power law, model B is blackbody + power law and model C is a disc blackbody + power law; all models include the effects of photoelectric absorption from material in the line of sight. Although the parameters of the models have limited physical significance, since the spectra are not of high enough quality

Table 2. Best fit parameters for models used to fit the PN 0.3–10 keV spectra of RX J0042.3+4115 in observations 1, 3 and 4; the letters (A, B, C) refer to the model used (as described in the text) and the numbers refer to the observation number. $N_{\rm H}$ is the equivalent line-of-sight column density of hydrogen (in cm^{-2}); kT is the blackbody temperature expressed in keV; $n_{\rm B}$ is the normalisation of the blackbody component: 10^{39} erg s^{-1} at 10 kpc for blackbody, $R_{\rm in}^2 \cos\theta$ for a disc blackbody of inner disc radius $R_{\rm in}$ observed at an angle θ; Γ is the spectral index of the power law component; $n_{\rm P}$ is the normalisation of the power law, in terms of photon cm^{-2} keV^{-1} s^{-1} at 1 keV. $F^{0.3-10}$ and $L^{0.3-10}_{760\rm kpc}$ are the unabsorbed flux and luminosity at 760 kpc respectively in the 0.3–10 keV energy band.

Model	$N_{\rm H}$ /10^{22}	kT	$n_{\rm B}$	Γ	n_P	χ^2/d.o.f.	$F^{0.3-10}$ /10^{-12}	$L^{0.3-10}_{760\rm kpc}$ /10^{37}
A1	0.18	...	...	1.66	$1.5\ 10^{-4}$	104/91	1.08	7.5
B1	0.25	1.69	$4.3\ 10^{-6}$	2.2	$1.75\ 10^{-4}$	102/89	1.22	8.5
C1	0.23	3.33	$2.4\ 10^{-4}$	2.2	$1.39\ 10^{-4}$	102/89	1.2	8.2
A3	0.16	...	...	1.79	$4.7\ 10^{-4}$	181/172	3.0	21
B3	0.25	1.32	$1.36\ 10^{-5}$	2.55	$5.65\ 10^{-4}$	162/170	3.8	24
C3	0.31	2.28	$3.59\ 10^{-3}$	3.32	$5.25\ 10^{-4}$	162/170	4.9	34
A4	0.18	...	...	1.82	$4.9\ 10^{-4}$	352/190	3.0	21
B4	0.23	1.23	$1.16\ 10^{-4}$	2.43	$5.09\ 10^{-4}$	229/188	3.4	24
C4	0.30	2.03	$5.79\ 10^{-3}$	3.4	$4.47\ 10^{-4}$	231/188	4.7	33

to discriminate between models, a reasonable fit to a spectrum will provide a good estimate to the 0.3–10 keV flux and luminosity. The best fit results are presented in Table 2. We obtain 0.3–10 keV luminosities of ∼8, ∼30 and ∼30 × 10^{37} erg s^{-1} in observations 1, 3 and 4 respectively. We see that Model A cannot fit the spectrum from observation 4, and thus must be be rejected for all observations. The average Galactic line of sight absorption in the direction of M 31 is 7×10^{20} atom cm^{-2} (Stark et al. 1992) while the modelled absorption of RX J00422.3+4115 is 20–30 × 10^{20} atom cm^{-2}, as seen in X-ray sources in M 31 (Kong et al. 2002). This suggests that RX J00422.3+4115 is indeed in M 31, or else has intrinsic absorption resembling the absorption found in M 31 by coincidence.

Leahy normalised (Leahy et al. 1983) power density spectra (PDS) with (5.2 s)$^{-1}$ resolution were obtained from the 0.3–10 keV EPIC lightcurves from observations 1, 3 and 4 using POWSPEC; the PDS were averaged over multiple spectra of 512 bins and the expected noise was subtracted; the PDS data were geometrically binned. The three power spectra are presented in Fig 3. We find that the PDS from all three observations are ∼ flat at low frequencies, and break to a steep power law at frequencies of ∼0.06–0.1 Hz. To establish the significance of the breaks, each PDS was modelled with both a simple power law and a broken power law. The parameters for the broken power law model were the cut-off frequency, $\nu_{\rm c}$, the power at that frequency, the index for frequencies lower than $\nu_{\rm c}$, α_1, and the index for frequencies higher than $\nu_{\rm c}$, α_2. Table 3 lists the parameters and goodness of fit of the two models for each PDS; clearly the simple power law model cannot acceptably fit any of the PDS, and all PDS are well fitted by the broken power law model, hence the PDS really do resemble those of low accretion rate binaries.

To establish whether the break is an artifact of the instrumentation, or inherent to RX J0042.3+4115, the PDS of seven bright X-ray sources identified with globular clusters by Kong et al. (2002) were examined; as they are likely to be high accretion rate neutron star binaries their PDS should not

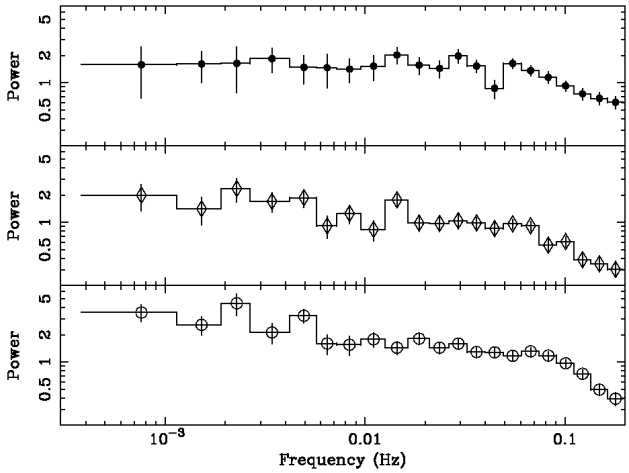

Fig. 3. Power density spectra of RX J0042.3+4115 from observations 1, 3 and 4 are displayed in the top, central and bottom panels respectively. The PDS of observation 1 is clearly flat below 0.04 Hz and a steep power law above 0.06 Hz, consistent with the PDS of low accretion rate XB (Wijnands & van der Klis 1999); indeed, a break is seen in the PDS of all three observations, below which the PDS is approximately flat.

Table 3. Fits of simple power law models (PLx) and broken power law models (BPLx) for observation x (1, 3 and 4); α_1 and α_2 are the spectral indices before and after the break frequency ($\nu_{\rm c}$). Numbers in parentheses are the uncertainties in the last significant figure.

Model	α_1	$\nu_{\rm c}$ (Hz)	α_2	χ^2/d.o.f.
PL1	−0.11(1)	...	...	21.8/11
BPL1	−0.04(2)	0.05(1)	−0.21(6)	5.8/9
PL3	−0.35(2)	...	...	62.2/11
BPL3	−0.24(3)	0.09(1)	−1.5(4)	8.6/9
PL4	−0.35(3)	...	...	45.7/11
BPL4	−0.27(4)	0.05(3)	−0.5(2)	13.7/9

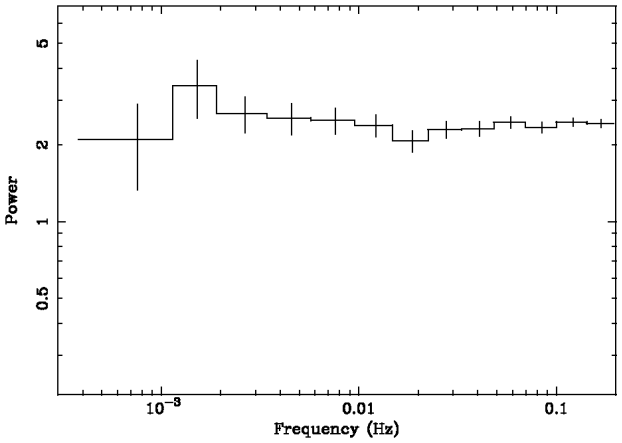

Fig. 4. The noise-subtracted PDS of the combined lightcurves of the seven X-ray sources associated with globular clusters used to search for an artificial break in the PDS; no break is seen.

contain a break in the observed frequency range. Although there is no reason to expect instrumental modulation of the true PDS that would produce the breaks we have observed, these checks were nevertheless made to be sure. For each globular cluster source, combined EPIC lightcurves from observation 4 were made and a PDS was obtained. Luminosities of the globular cluster sources were estimated from fits to PN spectra of simple power law models; the spectral channels were binned for a minimum of 20 counts per bin. Table 4 lists the best fit model parameters for the globular cluster sources. The luminosities of the globular cluster XB span $1-10 \times 10^{37}$ erg s^{-1}, hence we expect high accretion rate PDS with no breaks. No breaks were observed in the PDS of any of the globular clusters.

Additionally, a lightcurve was produced by summing all the EPIC lightcurves of the globular cluster sources; the intensity of this summed lightcurve is ∼1.5 count s^{-1}, (cf. 0.3–1 count s^{-1} for RX J0042.3+4115), hence the PDS had more than sufficient data to detect any instrumental break. The PDS of that lightcurve is presented in Fig. 4. A break in the PDS due to instrumental effects would be present in all PDS and so adding the lightcurves of several sources should make the break more prominent; in fact, fitting a simple power law to the combined globular cluster PDS resulted in a good fit (χ^2/d.o.f. of 0.6). A broken power law is not required to fit the globular cluster data. We can thus be confident that the PDS breaks we have observed are inherent.

6. Discussion

The power density spectra observed from RX J0042.3+4115 by XMM-Newton are flat with a break at <1 Hz, consistent with PDS from disc-accreting X-ray binaries XB at a low accretion rate, and inconsistent with PDS from high accretion rate XB (van der Klis 1989; Wijnands & van der Klis 1999). In LMXB with neutron star primaries, the characteristic low accretion rate PDS appear in the island state, the lowest luminosity state (van der Klis 1989); an example is 1E 1724−3045, an X-ray burster that exhibited a low accretion rate PDS at a few 10^{36} erg s^{-1} (Olive et al. 1998). The fact that RX J0042.3+4115 exhibits a low accretion rate PDS at luminosities exceeding 10^{38} erg s^{-1}, and that none of the globular cluster sources (likely LMXB with neutron star primaries) exhibit such PDS at luminosities of $0.1-1 \times 10^{38}$ erg s^{-1} strongly suggests that the primary in RX J0042.3+4115 is unlikely to be a neutron star. We conclude that the primary of RX J0042.3+4115 is a black hole candidate.

Since the argument rests on the luminosity of RX J0042.3+4115, it is important to be sure of its location in M 31. M 31 is located well out of the plane of the Milky Way, in a sparsely populated region of sky, meaning that RX J0042.3+4115 must be within our Galaxy, or in M 31 or a background AGN. We discount the possibility that RX J0042.3+4115 is an AGN and discuss possibilities where it is a local binary below.

AGN are powered by disc accretion onto massive black holes, so we might expect them to exhibit similar PDS, scaled to longer time-scales. Uttley et al. (2002) examined the PDS of four AGN (MGC-6-30-15, NGC 5506, NGC 3516 and NGC 5548) and found that the PDS of the first three are analogous to low accretion rate XB, but with the break at a few 10^{-6} Hz. These authors compare the PDS of these four AGN with that of the black hole XB Cygnus X-1 and conclude that the break frequency is related to the mass. The break frequency of RX J0042.3+4115 is several orders of magnitude higher than observed in these AGN and so we reject the possibility that it is a background AGN.

If RX J0042.3+4115 is actually a foreground object, then it probably belongs to the disc population and is located within ∼1 kpc. Hence the X-ray luminosity would be ∼6 orders of magnitude fainter, at $\sim 10^{32}$ erg s^{-1}, or fainter if closer than 1 kpc. We know from the PDS that RX J0042.3+4115 is powered by disc accretion, but this X-ray luminosity is several orders of magnitude too low for a persistent LMXB (Lewin et al. 1995). Hence RX J0042.3+4115 would have to be a cataclysmic variable (i.e. with a white dwarf primary) or a soft X-ray transient in quiescence.

All known Galactic cataclysmic variables have optical/UV counterparts (e.g Downes et al. 2001) and while RX J0042.3+4115 was associated with an optical source using the Einstein position (Trinchieri & Fabbiano 1991), the improved resolution of Chandra placed RX J0042.3+4115 away from any optical counterpart (Kong et al. 2002). The nearest object in the Haiman et al. (1994) optical catalogue is at $00^{\rm h}\,42^{\rm m}\,28^{\rm s}$ +41° 15′ 35.″7, i.e. just $5^{\rm s}$ away and has an apparent visual magnitude of $m_V = 20.075$. Hence an optical counterpart to RX J0042.3+4115 must be fainter than $m_V = 20$. A pessimistic estimate of the absolute visual magnitude for a non-magnetic CV is $M_V = 9$, considering only disc emission and an accretion rate of $10^{-11}\ M_\odot$ yr (Warner 1995); hence at 1 kpc, the apparent magnitude would be brighter than 19 and would have been seen in the Haiman et al. (1994) survey. Hence we can rule out the possibility that RX J0042.3+4115 is a normal non-magnetic CV. The observed spectra from RX J00422.3+4115 are consistent with Galactic magnetic CVs, but the X-ray luminosity at 1 kpc would be two orders of magnitude lower than normal. The system would have to be one of the theoretically

Table 4. A catalogue of point X-ray sources identified as globular clusters by Kong et al. (2002) and used to test the hypothesis that the break in the PDS of RX J0042.3+4115 is not instrumental. The best fit parameters of absorbed power law models to the spectra are given; the column headings have the same meanings as in Table 2.

Source	$N_{\rm H}$	Γ	$n_{\rm P}$	χ^2/d.o.f.	$F^{0.3-10}$	$L_{760}^{0.3-10}$	Break?
J 004212.1+411758	0.35	1.66	7.5×10^{-5}	97/114	0.54	3.7	N
J 004218.6+411401	0.13	1.55	1.29×10^{-4}	306/301	1.0	7	N
J 004226.0+411915	0.42	2.32	4.5×10^{-5}	56/73	0.22	1.5	N
J 004232.1+411939	0.21	2.06	7.4×10^{-5}	153/127	0.4	2.8	N
J 004259.6+411919	0.13	1.98	1.4×10^{-4}	275/250	0.78	5.4	N
J 004310.6+411451	0.10	1.74	2.12×10^{-4}	430/429	1.4	9.8	N
J 004337.2+411443	0.14	1.70	1.34×10^{-4}	268/241	0.93	6.4	N

implied, post period minimum CVs with a brown dwarf secondary (Kolb & Baraffe 1999).

If RX J00422.3+4115 is a local soft X-ray transient (SXT) in quiescence, its primary could be a neutron star or a black hole. SXTs typically brighten in X-rays by a factor of up to 10^7 over a week, then decay into quiescence over the course of a year; successive outbursts are usually separated by years to decades (see review in e.g. Tanaka & Shibazaki 1996). Observed spectra from SXTs in quiescence are often modelled using advection dominated accretion flow (ADAF) in the inner disc (e.g. Narayan et al. 1997; Sutaria et al. 2002). Since ADAFs are radiatively inefficient, a neutron star primary will radiate energy donated by accreting material impacting on the surface, while a black hole primary will simply swallow the accreting material; indeed quiescent neutron star SXTs have been observed to be 2 orders of magnitude brighter than quiescent black hole SXTs (Sutaria et al. 2002, and references within). Comparing the implied luminosity of 10^{32} erg s^{-1} for RX J00422.3+4115 with the known minimum luminosities of black hole and neutron star SXTs (Hameury et al. 2003), we find that if RX J00422.3+4115 was a local SXT, it would be likely to have a black hole primary.

Accepting that the RX J00422.3+4115 is a black hole binary in M 31, we must account for its being in the low accretion rate state at a luminosity as high as a few 10^{38} erg s^{-1}. The mostly likely explanation is that the low accretion rate state is limited to less than a certain fraction of $\dot{M}_{\rm Edd}$, the mass accretion rate corresponding to the Eddington limit, rather than $\dot{M}$ itself; hence RX 00422.3+4115 would only need to be more massive than a neutron star to allow a low accretion rate state at a higher accretion rate (observed luminosity). GS 1124-683 (Nova Muscae 1991) exhibited a low-accretion rate PDS at a 1.2–37 keV luminosity of $\sim 10^{38}$ erg s^{-1}, for a distance of 4 kpc (Miyamoto et al. 1993; Macomb & Gehrels 1999); the mass of the primary in this system has been determined to be $7.0 \pm 0.6\ M_\odot$ (Gelino et al. 2001), so in this case $\dot{M} \sim 0.1\ \dot{M}_{\rm Edd}$. Hence, a scenario in which RX J00422.3+4115 has a massive ($\sim 10\ M_\odot$) primary accreting at $\sim 0.1\ \dot{M}_{\rm Edd}$ is feasible and entirely consistent with the observed properties.

If the break frequency is related to the mass of the primary as supposed by Uttley et al. (2002), the similar break frequencies of Cygnus X-1 [0.04–0.4 Hz (Belloni and Hasinger 1990)] and RX J0042.3+4115 (0.05–0.09 Hz) suggests that the mass of the black hole in Cygnus X-1 [$10\ M_\odot$ (Herrero et al. 1995)] is similar to that in RX J0042.3+115, supporting the idea of a $\sim 10\ M_\odot$ black hole primary in RX J0042.3+4115.

To conclude, the three scenarios discussed for RX J0042.3+4115 are: that RX J0042.3+4115 is a post period minimum CV with a brown dwarf secondary; that RX J0042.3+4115 is a luminous black hole binary in M 31; that RX J0042.3+4115 is a local black hole SXT with intrinsic absorption imitating the absorption found in M 31. We consider that it is most likely to be placed in M 31. In this case, the system could be a microquasar, i.e. with a low mass companion; it would then be an analogue of the Galactic microquasar GRS 1915+105.

Acknowledgements. The authors would like to thank Carole Haswell for useful conversations and Andrew Norton for the code used to model the PDS. This work is supported by PPARC.

References

Belloni, T., & Hasinger, G. 1990, A&A, 227, L33
Belloni, T., Klein-Wolt, M., Méndez, M., van der Klis, M., & van Paradijs, J. 2000, A&A, 355, 271
Downes, R. A., Webbink, R. F., Shara, M. M., et al. 2001, PASP, 113, 764
Fender, R. 2002, in Relativistic Flows in Astrophysics, ed. A. W. Guthmann, M. Georganopoulos, A. Marcowith, & K. Manolakou, Lecture Notes in Physics, 589, 101
Frank, J., King, A. R., & Raine, D. 2002, Accretion Power in Astrophysics, 3rd Edition (Cambridge University Press)
Gelino, D. M., Harrison, T. E., & McNamara, B. J. 2001, AJ, 122, 971
Haiman, Z., Magnier, E., Lewin, W. H. G., et al. 1994, A&A, 286, 725
Hameury, J.-M., Barret, D., Lasota, J.-P., et al. 2003, A&A, 399, 631
Hasinger, G., & van der Klis, M. 1989, A&A, 225, 79
Herrero, A., Kudritzki, R. P., Gabler, R., Vilchez, J. M., & Gabler, A. 1995, A&A, 297, 556
Hjellming, R. M., & Johnston, K. J. 1981a, ApJ, 246, L141
Hjellming, R. M., & Johnston, K. J. 1981b, Nature, 290, 100
Homan, J., Wijnands, R., van der Klis, M., et al. 2001, ApJS, 132, 377
Jansen, F., Lumb, D., Altieri, B., et al. 2001, A&A, 365, L1
Kolb, U., & Baraffe, I. 1999, MNRAS, 309, 1034
Kong, A. H. K., Garcia, M. R., Primini, F. A., et al. 2002, ApJ, 577, 738
Leahy, D. A., Darbro, W., Elsner, R. F., et al. 1983, ApJ, 266, 160
Macomb, D. J., & Gehrels, N. 1999, ApJS, 120, 335

Miyamoto, S., Iga, S., Kitamoto, S., & Kamado, Y. 1993, ApJ, 403, L39
Narayan, R., Garcia, M. R., & McClintock, J. E. 1997, ApJ, 478, L79+
Olive, J. F., Barret, D., Boirin, L., et al. 1998, A&A, 333, 942
Osborne, J. P., Borozdin, K. N., Trudolyubov, S. P., et al. 2001, A&A, 378, 800
Spencer, R. E. 1979, Nature, 282, 483
Stark, A. A., Gammie, C. F., Wilson, R. W., et al. 1992, ApJS, 79, 77
Strüder, L., Briel, U., Dennerl, K., et al. 2001, A&A, 365, L18
Supper, R., Hasinger, G., Pietsch, W., et al. 1997, A&A, 317, 328
Sutaria, F. K., Kolb, U., Charles, P., et al. 2002, A&A, 391, 993
Tanaka, Y., & Shibazaki, N. 1996, ARA&A, 34, 607
Trinchieri, G., & Fabbiano, G. 1991, ApJ, 382, 82
Trudolyubov, S., Borozdin, K. N., Priedhorky, W. C., et al. 2002a, ApJL
Trudolyubov, S., Priedhorsky, W., Borozdin, K., Mason, K., & Cordova, F. 2002b, IAU Circ., 7798, 2
Trudolyubov, S. P., Borozdin, K. N., & Priedhorsky, W. C. 2001, ApJ, 563, L119
Turner, M. J. L., Abbey, A., Arnaud, M., et al. 2001, A&A, 365, L27
Uttley, P., McHardy, I. M., & Papadakis, I. E. 2002, MNRAS, 332, 231
van den Bergh, S. 2000, The galaxies of the Local Group, by Sidney Van den Bergh (Cambridge, UK: Cambridge University Press), Cambridge Astrophys. Ser., 35, ISBN: 0521651816
van der Klis, M. 1989, ARA&A, 27, 517
Warner, B. 1995, Cataclysmic Variables (Cambridge University Press), Chap. 4, p. 476
Wijnands, R., & van der Klis, M. 1999, ApJ, 514, 939